

Lab-scale experimental analysis of the cyclic compaction-recovery characteristics of uncured thermoset prepreg

Margarita Etchegaray Bello, Ralf Engelhardt, Dennis Bublitz & Klaus Drechsler

To cite this article: Margarita Etchegaray Bello, Ralf Engelhardt, Dennis Bublitz & Klaus Drechsler (2022) Lab-scale experimental analysis of the cyclic compaction-recovery characteristics of uncured thermoset prepreg, *Advanced Manufacturing: Polymer & Composites Science*, 8:2, 56-67, DOI: [10.1080/20550340.2022.2064069](https://doi.org/10.1080/20550340.2022.2064069)

To link to this article: <https://doi.org/10.1080/20550340.2022.2064069>



© 2022 The Author(s). Published by Informa UK Limited, trading as Taylor & Francis Group.



[View supplementary material](#)



Published online: 28 Apr 2022.



[Submit your article to this journal](#)



Article views: 1071



[View related articles](#)



[View Crossmark data](#)

Lab-scale experimental analysis of the cyclic compaction-recovery characteristics of uncured thermoset prepreg

Margarita Etchegaray Bello, Ralf Engelhardt, Dennis Bublitz and Klaus Drechsler

Chair of Carbon Composites, TUM Department of Aerospace and Geodesy, Technical University of Munich, Garching, Bayern, Germany

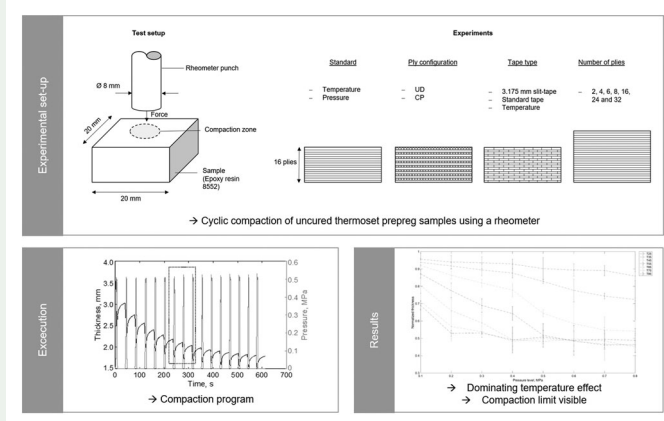
ABSTRACT

During its consolidation, uncured thermoset prepreg is exposed to cyclic loading conditions throughout the various stages of the process chain, including material deposition, vacuum debulking, and curing. One significant challenge involves understanding multilayer prepreg tapes' compaction behavior to optimise the process's efficiency and improve the final laminate properties. Automated Fibre Placement (AFP) is a suitable process for the automated manufacture of high-quality aerospace structures with reproducible properties. The compaction analysis offers the potential to reduce subsequent steps during other related compaction stages in the process, such as vacuum debulking or autoclave curing. A cyclic compaction-recovery test that approximates AFP conditions was performed with a rheometer. An experimental analysis was conducted into different parameters' qualitative influence on uncured multilayer thermoset prepreg samples' compressibility and their characteristics during load release, using a rheometer on a laboratory scale. The variables manipulated were: temperature, pressure, the number of plies, ply configuration, and tape type. The results showed that temperature strongly influenced the thickness reduction until a compaction threshold was approached, and the pressure level's effect on the final thickness depended greatly on the temperature. The thickness reduction was greater at higher temperatures until a compaction threshold was observed. Further investigations are recommended to gain insight into the flow mechanism within the sample and its void content after compaction to use the data to optimise the parameters.

KEYWORDS

AFP; consolidation; prepreg; thermoset

GRAPHICAL ABSTRACT



Introduction

Cyclic loading processing conditions of uncured thermoset prepreg are present during its process chain, especially throughout the consolidation of the material. A good understanding of the material behavior throughout the process stages is necessary to exploit these capabilities further. Automated

manufacturing of composite structures offers advantages over manual layup in terms of reproducibility and efficiency. Automated Fibre Placement (AFP) is an established process for automated prepreg deposition, increasing process robustness and the deposition rate. Although the process was initially established to reduce debulking operations, it is still

CONTACT Margarita Etchegaray Bello  margarita.etchegaray.bello@tum.de  Chair of Carbon Composites, TUM Department of Aerospace and Geodesy, Technical University of Munich, Boltzmannstr. 15, D-85748, Garching, Bayern, Germany

 Supplemental data for this article can be accessed online at <https://doi.org/10.1080/20550340.2022.2064069>.

© 2022 The Author(s). Published by Informa UK Limited, trading as Taylor & Francis Group.

This is an Open Access article distributed under the terms of the Creative Commons Attribution License (<http://creativecommons.org/licenses/by/4.0/>), which permits unrestricted use, distribution, and reproduction in any medium, provided the original work is properly cited.

not capable of carrying out this objective [1, 2]. Composite manufacturing processes are influenced by the complex relationships between the composite systems' matrix and fibres. Thus, the material properties have been studied in the literature to optimise the process design and make better predictions about the material behavior during processing [3].

The compaction behavior of prepreg plies is crucial as it influences the formation and retention of voids, the fibre volume fraction, and fibre waviness [1]. Although a major part of the compaction for thermoset prepreg laminates is realised during autoclave curing, initial compression is applied during the deposition, for AFP *via* the compaction roller as part of the placement head. Consequently, the layup process is typically interrupted by regular intervals of vacuum debulking after a certain number of plies. During the debulking process, further compression is applied to the material.

The deformation and flow behavior of the prepreg systems is influenced by the conditions applied. One of the main causes of the system's complex relationship is its flow mechanisms. Toughened prepreg systems, combining thermoset matrix with thermoplastic additive particles, lead to a complex combination of both low-viscosity thermoset and high-viscosity thermoplastic flow mechanisms. Such behavior appears during the AFP process while the material is being consolidated. These flow behaviors manifest as bleeding and squeezing. The former occurs at low viscosity, where resin flows relative to the fibres. The latter at high viscosity, causing the entire fibre-matrix system to move transversely to the compaction direction [4, 5]. Diverse studies have been carried out, driven by the need to understand the compaction behavior of composite materials, mainly due to the complex interaction between the fibres and the matrix to explain the deformation and flow mechanisms within the material.

Blößl and Schledjewski [3] investigated the compaction behavior of plant-fibrous reinforcements under diverse parameters, including fabric type, the number of layers, loading and load-release cycles, and compression rate. The experimental data was further used to fit an empirical model that shows overall better agreement than the traditional power and exponential law models.

Moreover, several works have been carried out to gain an insight into the fundamental compaction behavior of prepreps. Hubert and Poursartip [6] analysed the flow and compaction of carbon-epoxy angle laminates during the curing process. Two different systems were analysed, AS4/3501-6 and AS4/8552, under distinct layup configurations, bagging conditions, and tool geometries. Gutowski and Dillon [7] analysed the deformation of wet carbon

fibre bundles and compared the diverse available to the 3D model previously proposed by Cai and Gutowski [8]. The model showed a good agreement with the studied data, finding a 'universal' model fit for bundle compression.

Nevertheless, research on the material's compressibility under AFP conditions is limited. In the few studies carried out, the AFP process was simulated employing various test mechanisms, such as mechanical testing machines [1], dynamic mechanical analysers [5, 9], and rheometers [10]. Furthermore, multiple studies investigated the consolidation of the prepreg materials using experimental and numerical approaches for the different AFP consolidation stages, such as layup [5, 9, 10], debulking [5, 11], and autoclave curing [5, 12, 13].

Lukaszewicz and Potter [1] studied the displacement and temperature dependence on uncured M21/IMA prepreg compression. They aimed to obtain a viscoelastic and elastic-plastic material description to help select an appropriate model for the uncured prepreg's compression. Ivanov et al. [9] analysed the compression behavior of M21/IMA prepreg for AFP processing conditions under the varied temperature (30–90 °C), ply configuration, unidirectional (UD) and cross-ply (CP) stacks, and loading regimes (slow monotonic and ramp dwell). Posterior research done by Nixon-Pearson et al. [5] complemented the study mentioned above and involving other parameters, such as the size and weight of the plies. They also carried out the experiments to increase the force from 20 to 60 N in 1200 s, with five time-stages of 240 s and 10 N each. Moreover, they implemented different sequences of stacks that included CP, block-ply (BP), and semi-block-ply (SB), as well as an additional type of prepreg (8552/IM7). They reported the presence of a compaction limit, where no further thickness reduction was observed above certain conditions. Sorba et al. [14] studied the compaction behavior of UD uncured thermoset prepreg (HexPly M21) below 80 °C and at less than 30 min to avoid curing the samples. This temperature range helps in avoiding resin bleeding and generate pure squeeze flow. During their experiments, the samples' initial and final thicknesses were registered. Additionally, insight into the plies' movement and their alignment to the fibre orientation suggested a resin flow perpendicular to the fibre direction and in-plane rotation as well as the bending of the plies.

Lichtinger [10] analysed the thickness evolution of UD and multidirectional (MD) samples of HexPly 8552 prepreg under various processing conditions. His work employed eight cycles using a rheometer to evaluate the compaction and material

Table 1. Overview of all experiment parameter variations.

Test type	Material	No. of plies	Fibre orientation	Temperature (°C)	Pressure (MPa)
Full-factorial	8552/AS4	16	UD	25/35/45/55/ 65/75/85	0.1/0.2/0.3/0.4/ 0.5/0.6/0.7/0.8
Fractional-factorial		2/4/8/16/24/32	UD	55	0.5
Fractional-factorial		16	CP	55	0.5
Fractional-factorial	8552/IM7 (slit-tape)	16	UD	25/55/85	0.5

recovery. Temperature, pressure, compression time, and release time were varied.

Due to the influence of compaction on the processing of various fibre-reinforced polymer (FRP) materials, it is crucial to understand the fundamental behavior of the material itself. Furthermore, investigating the materials' compaction behavior can also help derive relations between processing parameters and the resulting properties [3].

Compaction during placement is important to guarantee a defined state of fibre orientation. Furthermore, the high reproducibility of layup and compaction by AFP offers the potential to reduce the extent of vacuum debulking and potentially even autoclave curing [11, 15]. Thus, this study focuses on the compressibility of the material, approximating layup conditions in a controlled environment, where the fundamental behavior of the material and the influence of different parameters can be observed.

In the literature, the consolidation of prepreg under AFP processing parameters focusing on its cyclic boundary condition and sample recovery response is still open. The novel lab-scale experimental method developed by Lichtinger [10] was adapted to extend the limited repetitions and include additional parameter variations. The effect of the compaction time was not significant for shorter periods, and the release time showed only minor influence on the thickness reduction. As a result, the main aim of this study is to analyse the influence of pressure and temperature in AFP processing conditions on the compaction behavior of uncured prepreg laminates in a full-factorial study design. The second set of parameters was also included in the study to gain further insights into additional important variations of the AFP process, such as the number of layers, layer configuration, and tape type. The effect of the number of plies, the fibre orientation, and the material type were determined on a fractional-factorial sample base. Small samples of uncured stacked prepreg layers were subjected to cyclic compactions in a rheometer, allowing high reproducibility at low noise in lab conditions and efficient sample testing. The results can help understand the fundamental material behavior during consolidation to optimise AFP process parameters toward fewer vacuum debulking cycles.

Materials and methods

Equipment

The compaction tests were carried out using a modular *Anton Paar MCR302* compact rheometer with an additional *Anton Paar Viscotherm VT2* cooling system. An adapted sample tray with increased wall thickness was used to avoid tray deformation leading to thickness measurement distortions. A cylinder (without a bevelled edge) with a cross-section of 8 mm was used as a rheometer punch. The rheometer can apply controlled compressive forces up to 50 N, resulting in a maximum applicable pressure of 1 MPa for this setup.

Material and sample preparation

The samples consisted of toughened aerospace-grade unidirectional (UD) prepreg. For the full-factorial main set of experiments, HexPly® 8552/AS4 by Hexcel was used. The material system has a nominal cured ply thickness of 0.130 mm, a nominal fibre volume fraction of 57.42%, and a nominal resin content of 35% weight [16]. The slit-tape samples included in the fractional-factorial set of experiments consisted of Hexcel HexPly® 8552/IM7 3.175 mm width slit-tape as used for AFP processing. This system has a nominal cured ply thickness of 0.131 mm, a nominal fibre volume fraction of 57.70%, and a nominal resin content of 35% by weight [16]. The difference between the AS4 and IM7 fibres limits direct comparison of the results. However, studies presented in the literature for multi-ply compression experiments found that systems' compression strengths for AS4 and IM7 fibres were similar when the same matrix (3501-6) was used [17].

All samples were manually laminated and tested in an uncured state with a max. test duration of 20 min at max. 85 °C, in a range without any significant influence on the degree of cure [16]. The samples have a size of 20 × 20 mm with 16 plies for the standard-setting. Oversized plies were stacked *via* manual layup and subsequently cut to the final size using a *Zünd M-1200 CV* digital cutting system. A 50% staggering was incorporated in between plies for the slit-tape samples. It must be considered that the influence of the variation due to manual layup is out of this work's scope. The samples were placed on the protective backing paper that came with the

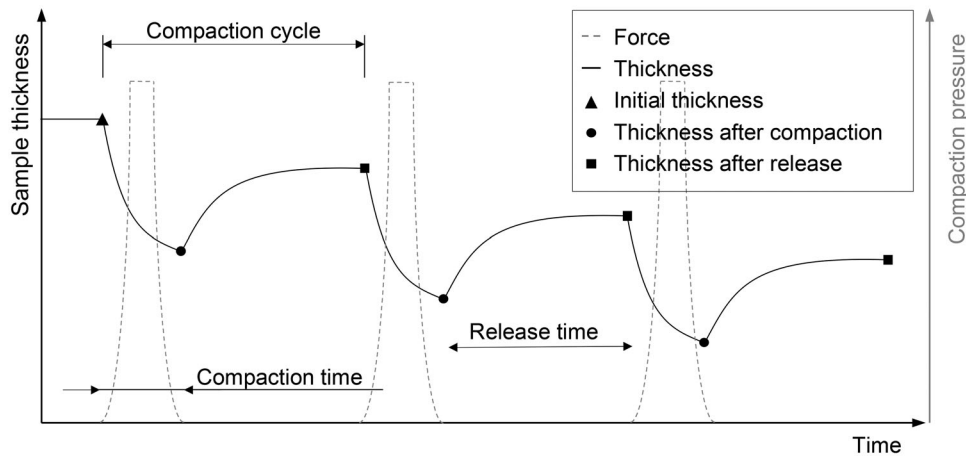


Figure 1. Thickness and pressure profile of the rheometer compaction experiments showing three exemplary cycles replicating the compaction profile of AFP.

material. Additionally, a polymer film was placed on top to cover the samples and avoid measurement effects due to the tackiness of the sample and the rheometer punch. The effect of the paper and polymer film during the compaction tests can be neglected, as it composes less than 3% of the samples' thickness. The compaction response of these components was analysed over three cycles in separate compaction trials, showing no significant thickness effect for compaction or release with the given measurement accuracy.

Experimental procedure

A full-factorial set of experiments was implemented with the rheometer running in force-controlled mode and with the main parameters, (i) pressure and (ii) temperature (cf. Table 1). In addition, the influence of (iii) the number of plies, (iv) fibre orientation, and (v) material type was investigated on a fractional-factorial sample basis. For all sets, the samples were exposed to several compaction cycles replicating the compaction profile during the deposition in the AFP process as developed by Lichtinger [10]. The number of compaction cycles applied corresponded to the samples' number of layers to approximate AFP processing conditions. Nevertheless, this approach limits the direct comparison with the AFP process due to the bulk compaction of the sample. Each layer experiences additional compression during the AFP process after a subsequent layer is deposited.

A compaction cycle includes a compaction time of 3 s, followed by a release time of 30 s (cf. Figure 1). These time ranges were selected to gain insight into the material behavior during compaction and release conditions within the limitations of the rheometer regarding compaction time capabilities and the minimum time required for a stable and repetitive execution of the test procedure due to the loop-

function used to control the rheometer. Although the compaction time can reach the centisecond range during the AFP process, the study presented by Lichtinger [10] performed a parametric analysis with variations in the compaction and release times. The results showed no influence of the compaction time on the qualitative compressibility behavior when the time was reduced to 1 s. Similarly, the influence of the diverse release time parameters could be neglected since the most significant reduction was during the first second. The closed rheometer tray with the sample was first heated up to the desired test temperature for 300 s to ensure a homogeneous temperature¹. The initial thickness of the sample was then measured by contacting it with the rheometer punch with a force of 0.1 N. After this initial measurement, a loop with the respective amount of compaction cycles was started. The rheometer punch was lowered at a rate of 90 $\mu\text{m/s}$ – corresponding to the max. displacement rate that the rheometer could achieve until the desired force was reached. Points of interest were (i) the initial thickness, (ii) the thickness after compaction, and (iii) the thickness after release. The data was processed for analysis with MATLAB. Random overloads, attributed to the high sampling rate of the experiments, led to a negligible number of missing points in the thickness profile that were filled with linear interpolation. The single loop segments were assembled, mean values for each parameter variation were calculated, and the thickness values were normalised to their initial thickness for better comparison. Each parameter variation was repeated three times. The raw data is published on the mediaTUM [18] data repository.

¹An additional experiment was devised to determine the time needed for the sample to heat. A *Pico Technology TC-08* thermocouple was connected to the upper surface of the sample to measure the required time to reach a temperature of 85 °C when placed on the rheometer hood. The resulting time was approximately 4 min.

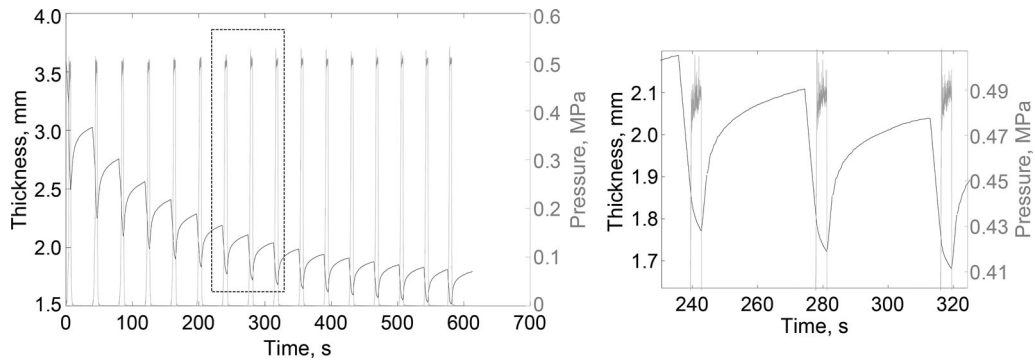


Figure 2. Exemplary thickness and compaction pressure profile of a 16-cycle compaction program with $T = 55^\circ\text{C}$, $p = 0.5\text{ MPa}$ (left) and a zoom-in (1.6x for the pressure and 7x for the time) of the selected area (right) for a better visualisation of the relation between the thickness and compaction pressure during two cycles.

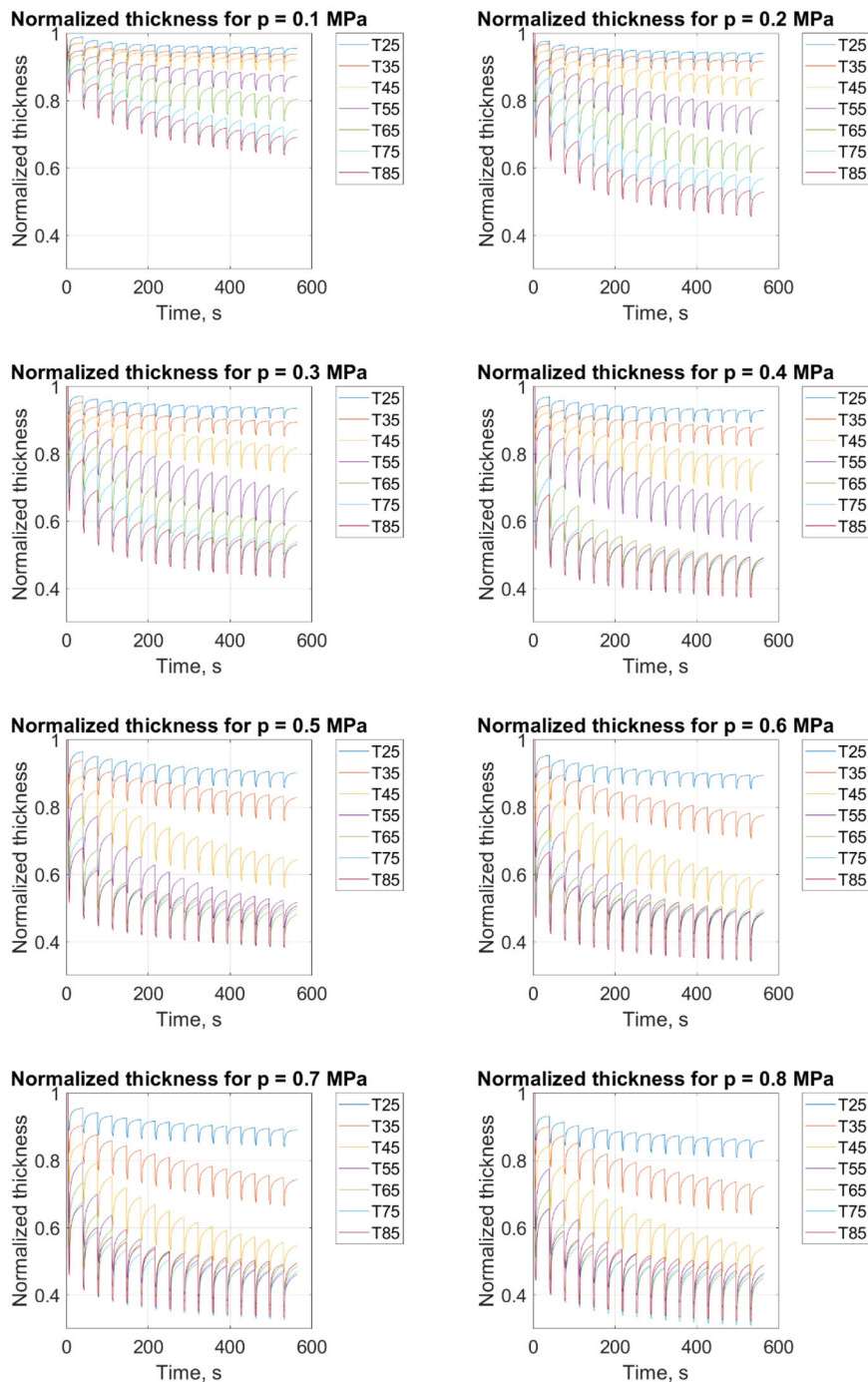


Figure 3. Normalised thickness over 16 cycles at different compaction pressure and temperature levels, respectively.

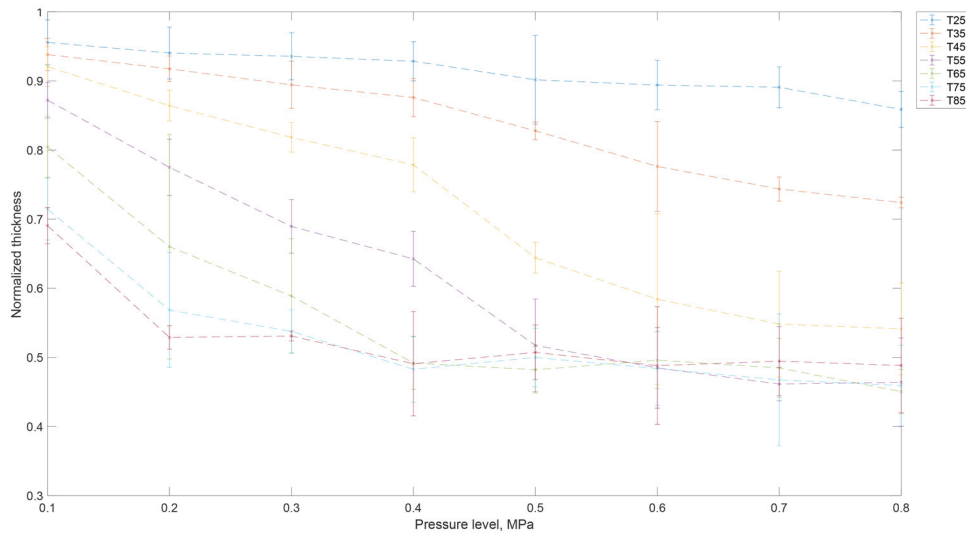


Figure 4. Normalised thickness comparing the final thickness after 16 compaction cycles to the initial thickness for different temperature and pressure levels.

Furthermore, specific samples were analysed with the *Olympus BX41M-LED* microscope to gain insight into the compression behavior. The selected samples were subjected to a soft-curing program, as described by Engelhardt et al. [19], to maintain their compacted state before examining them with the microscope. Additionally, the samples' porosity and void size were calculated using the software of the microscope.

Results and discussion

Figure 2 presents the actual thickness and force profile of an exemplary standard experiment with 16 compaction cycles. The uncured prepreg laminate shows viscoelastic material behavior due to its time-dependency. The thickness increases with the release of the compaction pressure revealing elastic recovery.

Effects of pressure and temperature

During the main set of experiments, the pressure and temperature were varied in a full-factorial design. Figure 3 shows the average sample thickness normalised by its initial value during the 16 compaction cycles for the different compaction pressure and temperature levels. The viscoelastic behavior is observed at all studied conditions. Additionally, the normalised thickness decreases with the temperature and the number of compaction cycles for all experiments. For all samples, the highest recovery is observed during the first cycle.

The terms 'compaction limit' and 'degree of compaction' as defined by Ivanov et al. [9] are used in this work. The former denotes the convergence of the thickness curves above a certain pressure or temperature, where no further compaction is observed. The degree of compaction corresponds to the final thickness of each sample, including those that did not reach a compaction limit.

The results show that for 0.1 MPa compaction pressure, the thickness reduction increases over the entire range of temperature levels. The greatest thickness reduction – to 69% of the initial thickness – appears at 85 °C after the 16th compaction cycle. For temperatures below 55 °C, the thickness plateaus toward the last cycles, reaching a degree of compaction between 65% and 75%. For temperatures of 55 °C and above, no such plateau can be seen at this pressure level. The biggest relative effect of a temperature increase can be seen from 55 °C to 65 °C, where the relative difference is up to 11.8%. The thickness profiles at 0.2 MPa show similar low compaction below 45 °C. The greatest thickness reduction occurs again at 85 °C after 16 cycles, with a normalised final thickness of 52.8%. Based on the thickness profile, it is assumed that from this pressure level, the compaction limit is achieved at 85 °C. It is not easy to make a clear distinction at high temperatures due to the standard deviations of the final thickness (cf. Figure 4). However, it is assumed that the compaction limit at 85 °C already exists for this pressure level. The temperature differs from the temperature reported by Ivanov et al. [9], where the compaction limit was reached at approximately 60–70 °C and at a pressure of 0.26 MPa with 18-ply samples of M21/T700. The final thickness reduction at the compaction limit is similar (~50%). The normalised final mean thickness reduction obtained for the studied material at 0.26 MPa by linear interpolation at 65 °C is 61.7%. Nevertheless, the compaction limit observed in this work is around 10% lower. The thickness profile obtained for 0.26 MPa for the temperatures of 75 °C and 85 °C converge to similar values with only 1.9% of the final thickness difference. Hence, the compaction limit is achieved at 75 °C for this pressure level. This is in good agreement with the result of Nixon-Pearson et al. [5], showing that the

compaction limit is independent of the temperature above a specific temperature. The temperature threshold for their test conditions was found at 70 °C, i.e. the viscosity of the material did not influence its compressibility above these conditions.

For 0.4 MPa, the compaction limit is reached at 65 °C after the 11th cycle. The thickness reduction for 65 °C and all temperatures above converge to approximately 49% of the initial thickness. For 0.5 MPa and above, the maximum thickness reduction stabilises around 50%. The compaction limit is already reached at a temperature of 55 °C.

Figure 4 summarises the normalised overall thickness for all temperature and pressure variations, including their standard deviation. Clearly, the effect of increased pressure on the compaction is small for low temperatures of 25 °C and 35 °C. The temperature threshold by which the compaction limit is reached varies with the pressure applied. A higher compaction pressure decreases the required temperature to achieve the compaction limit. Once the compaction limit is reached, the increase in temperature, pressure or cycles does not lead to any further compression for the setup given.

Comparable lab-scale compaction studies by Ivanov et al. [9] and Nixon-Pearson et al. [5] show a compaction and transverse widening limit corresponding to the onset of bleeding. This effect was attributed to the transition from squeezing to bleeding flow from 60 °C to 70 °C at a pressure of 0.26 MPa.

The effect of the (i) temperature, (ii) pressure, and the (iii) interaction between them on the final thickness of the sample was studied using a two-way Analysis of Variance (ANOVA). The results showed that all three criteria significantly influence the resulting sample thickness for a confidence interval of 95% ($p < .05$).

The present results show that a general compaction limit is reached when the experiment conditions are 55 °C and 0.5 MPa, with around 50% thickness reduction compared to the initial thickness value (cf. Figure 4). Once the compaction limit is reached, the thickness becomes independent of the temperature, pressure or cycles. It was suggested by Ivanov et al. and Nixon-Pearson et al. [5, 9] that this represents the onset of bleeding. This effect may be observed in Figure 3 for the different pressure levels, where the slope of the thickness curves drastically changes after the compaction limit is reached. After the compaction limit is reached, the cycles may produce more bleeding flow of the resin into the lower-pressure non-consolidated region of the specimens. This effect was studied by conducting a test with a bigger rheometer punch to ensure that the whole specimen was compacted (cf. Supplementary material). The material's compressibility was lower than the sample with unconsolidated

regions. This suggests that bleeding flow may be favored using a smaller rheometer punch. This effect may be comparable to the AFP processing conditions, where the nip point of the compaction roller is smaller than the laminate, and thus, may enhance bleeding flow to the unconsolidated regions.

Specific samples were further analysed on a microscopic scale to gain additional insight into the influence of pressure and temperature on the material's compressibility and void fraction. The results are presented in Figure 5: the untested specimen (denoted as reference), 0.5 MPa and 55 °C, 0.1 MPa and 25 °C; 0.1 MPa and 85 °C, 0.8 MPa and 25 °C, and 0.8 MPa and 85 °C. The compacted area is represented by half of each sample to allow a better comparison between a pair of specimens. In contrast to the expected results, the void fraction of the samples does not directly correlate to the final thickness reduction. Figure 6 presents a zoom-in of the compacted area of the sample to visualise this effect. The void fraction calculated using the microscope software for the specimens' section shown in Figure 6 is presented in Table 2. The porosity was reduced using the lowest temperature level and increased for 55 °C and 85 °C. The lowest porosity ratio was observed for the lowest temperature and the highest pressure, whereas the highest porosity was observed for both maximum temperature and pressure levels.

As previously suggested, this phenomenon may be attributed to the flow mechanisms within the samples. It is assumed that increasing temperature lowers the viscosity and may lead to bleeding flow. Once the compaction limit is reached, further cycles may increase the void content within the consolidated section. So, depending on the number of layers, it would be recommended to consider this limit to avoid further cycles after this limit is present. Under this assumption, using lower temperatures favors squeezing flow. Nevertheless, to allow enough compaction, the pressure needs to be increased. Therefore, it would be important to investigate the influence of compressibility and pressure on the consolidation flow mechanisms to select the adequate parameters during processing and favor squeezing flow during the layup.

Hence, it can be recommended to study the effect of compaction under actual AFP conditions to gather more information about the correlation between compressibility and voids within the samples to select adequate consolidation conditions.

Effect of the number of plies

In addition to the full-factorial variation of pressure and temperature, single factors such as the specimens' layer number were varied in a separate set of

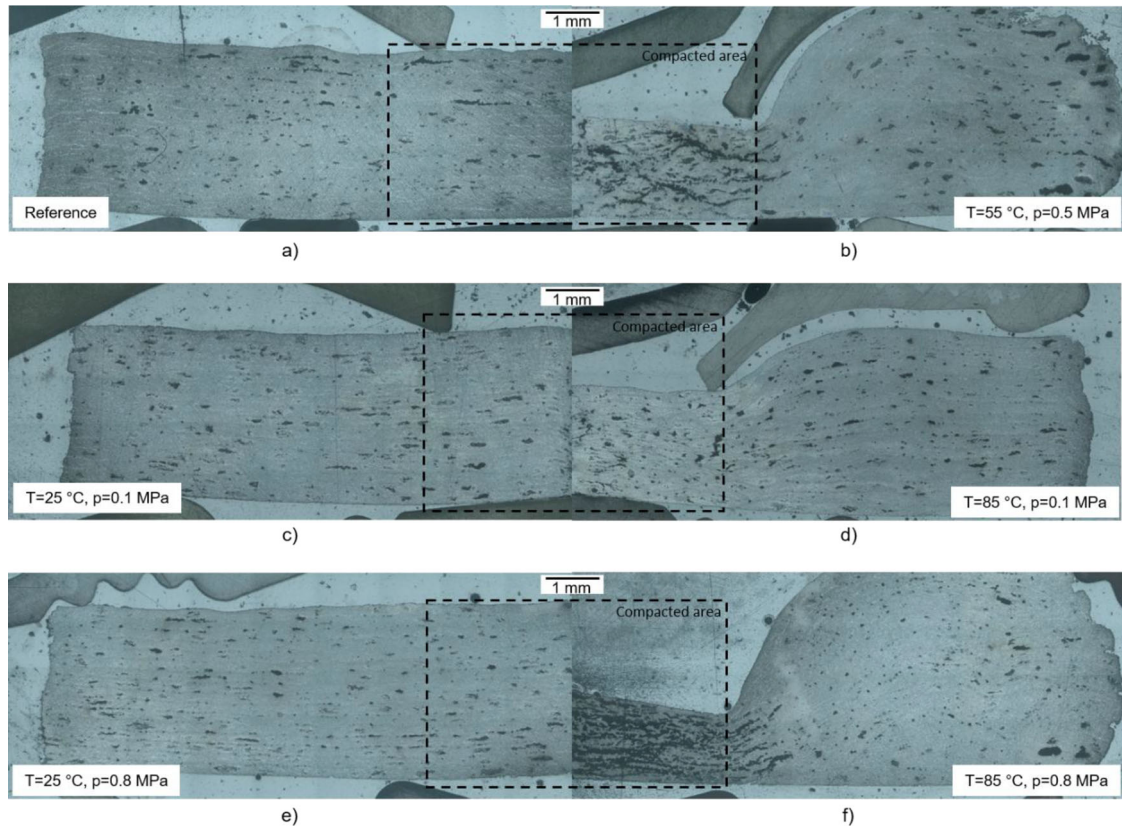


Figure 5. Samples' compacted area (---).

experiments. The tests were performed at 55 °C with a pressure of 0.5 MPa and UD layup (cf. Table 1). In Figure 7, the thickness profile for the compaction of samples with 2, 4, 8, 16, 24, and 32 plies is shown with normalised (left) and absolute (right) thickness values. Although the samples with a different number of layers had a different initial thickness, it is possible to observe that they all present a similar qualitative thickness profile. The normalised thickness of the samples (cf. left side of Figure 7) shows that the specimens composed of more layers were more prone to experience higher compaction during the initial cycles. This effect is attributed to the air between the plies and the several layer-to-layer interfaces. The highest difference after the second cycle between the 2-ply and 32-ply samples lies around 15%. Above 8-ply samples, the normalised thickness converges to a similar compaction ratio after the cyclic compaction program. The general progress of the compaction is similar (cf. left side of Figure 7). Hence, the simplification of the bulk compaction instead of layer-by-layer compaction seems to be adequate for this work. The number of layers influences the absolute thickness profile, even though the normalised thickness follows a similar qualitative behavior and converges to a comparable limit independent of the stacks' number of layers. The ANOVA showed that the number of plies does not significantly influence the final normalised thickness ($p < .05$).

The time per cycle increases with ply number due to force-controlled programming of the

rheometer. Higher absolute sample thicknesses lead to longer travel distances to reach a specific reaction force. After high compaction ratios during the first cycles, it converges toward the compaction limit. With an increased number of cycles, the compaction per cycle decreases. For the 16-ply samples, the mean thickness reduction compared to the previous cycle was around 1% for the last two cycles. They experienced only 0.5% to 0.7% compaction after the 12th cycle. For the 32-ply samples, this compaction value was reduced to 0.4% after the 12th cycle. Compared to the initial thickness, the final normalised thickness was 51.7% for 16 plies, 46.1% for 24 plies, and 45.7% for 32 plies. The compaction limit explains this behavior. The increase of layers, and thus, cycles – for the current setup – leads to more cycles, where the thickness does not further decrease.

Effect of the fibre orientation

The influence of the fibre orientation was analysed for the samples with cross-ply (CP) fibre orientation to the standard UD samples. The tests were performed at 55 °C with a pressure of 0.5 MPa (cf. Table 1). The compaction profile (cf. Figure 8) shows much higher UD laminate compaction than the CP samples. The UD samples were compacted to 48.2% of their initial thickness, whereas the CP samples maintained 84.0% of their initial thickness. As expected, the ANOVA showed that the configuration significantly influences the final normalised thickness ($p < .05$).

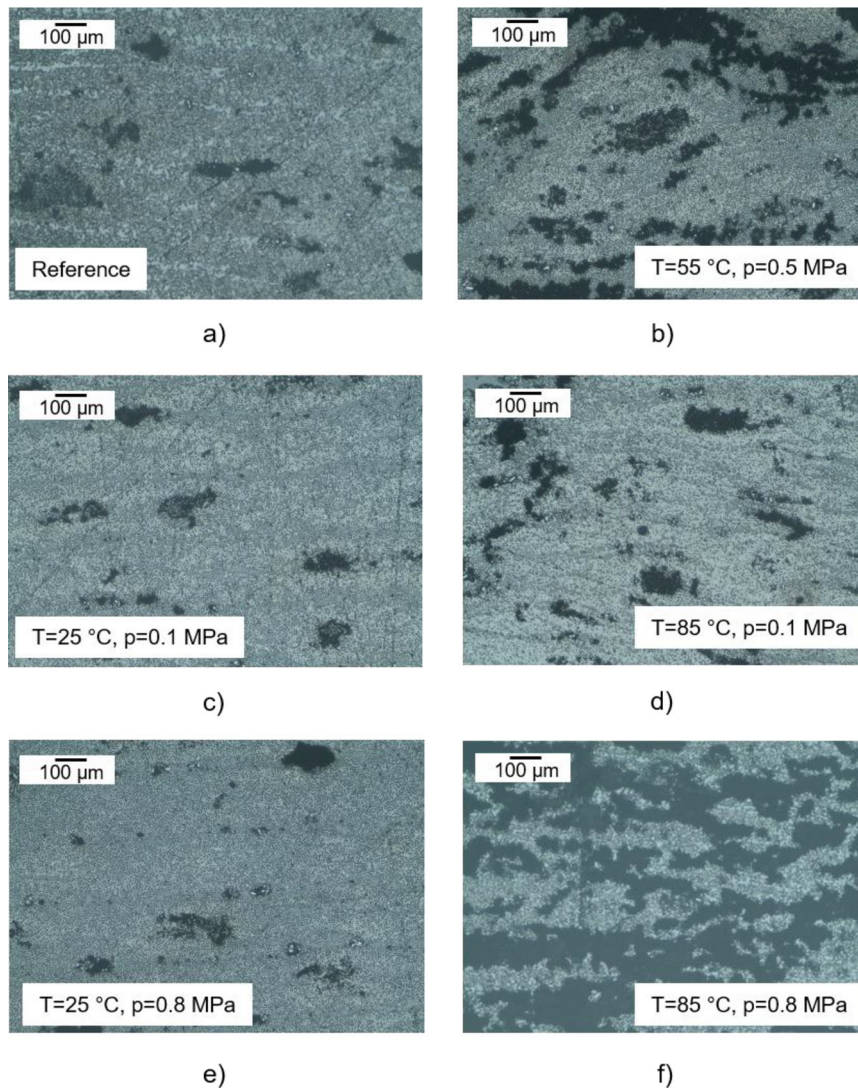


Figure 6. Zoom-in (10x magnification of Figure 5) of the compacted area.

Table 2. Porosity values of the samples analysed using microscopy.

Sample	Temperature (°C)	Pressure (MPa)	Porosity (%)	Max. void size (μm)
a)	Reference	Reference	8.58	333.82
b)	55	0.5	31.99	1047.58
c)	25	0.1	6.40	348.88
d)	85	0.1	17.40	503.36
e)	25	0.8	5.41	217.85
f)	85	0.8	60.86	1626.39

These results correspond to other studies showing much higher UD laminates compaction than non-UD layup [5, 9, 10]. Non-UD plies are isolated, especially transverse widening, and reach a locking configuration earlier than UD plies [5].

Effect of material and tape type

The standard samples of this set of experiments consist of unslit prepreg sheet material. Here, slit-tape samples were compared to the standard samples to analyse the influence of the tape geometry with regard to the AFP process. The slit-tapes had a

width of 3.175 mm and were manually placed, as described in the methodology section.

Figure 9 shows the compaction profiles of standard (STD) and slit-tape (SLT) samples at three different temperatures. At 25 °C, the profiles are well aligned, showing only minor differences in the release response. The initial thickness is reduced to about 90% for both tape types. At 55 °C, the slit-tape samples experienced less compaction than the standard samples. They were reduced to 54.4% of their initial thickness compared to 51.8% for the standard setup. There is a considerable divergence of the profiles for the highest temperature level. The slit-tape samples were compacted to 39.2% of their initial thickness, the standard samples to 50.8%. There is no clear trend visible with rising temperature. One possible explanation is a difference in the compaction limits of the different sample setups. As described in the full-factorial variation of temperature and pressure above, the standard samples reach a compaction limit at 55 °C and 0.5 MPa pressure. There is only a minor thickness reduction beyond the compaction limit. The slit-tape samples

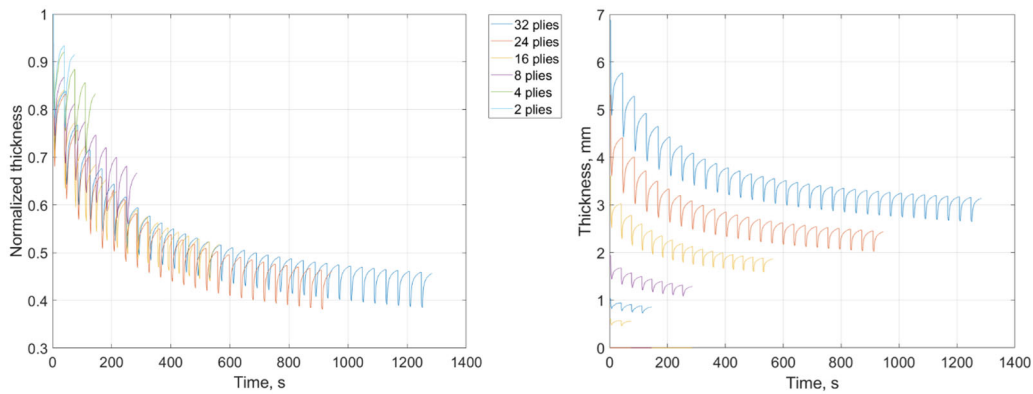


Figure 7. Compaction profile of samples with different ply numbers with normalised (left) and absolute (right) thickness profile.

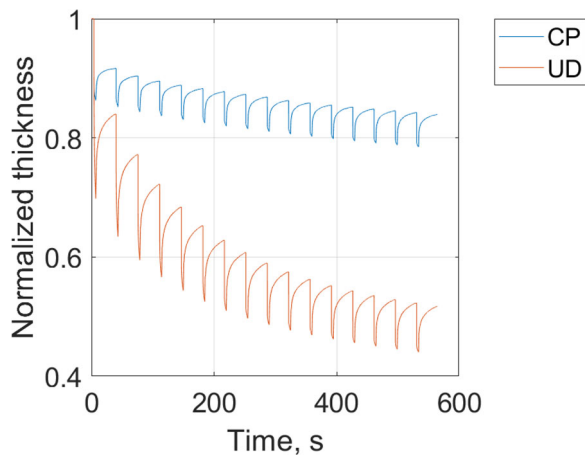


Figure 8. Normalised compaction profile of samples with cross-ply (CP) and unidirectional (UD) fibre orientation.

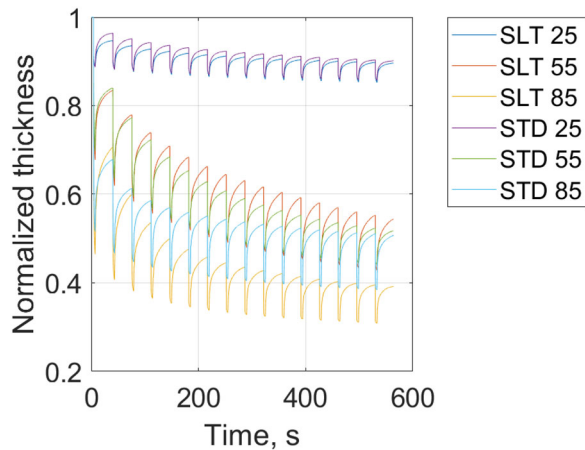


Figure 9. Normalised compaction profile of standard (STD) and slit-tape (SLT) material samples at different temperatures.

experience significant additional compaction at 85 °C, so it seems they have a compaction limit at a higher temperature–pressure–combination. This phenomenon can be attributed to the width of the tapes, as the space between two slit-tapes could allow for further transverse widening of the individual tapes. It is crucial to consider this aspect since a scale-up of the experiment could be exploited during the actual process to achieve higher compaction.

Relevance for the AFP process and main limitations

Understanding the material's fundamental compaction behavior during layup can help to gain insight into the dominant process parameters and their effect on the compaction behavior. The present study is focused on analysing the qualitative compaction characteristics under similar boundary conditions yet under a controlled environment.

Among the primary outcomes of the study and their application into the actual process, the following observations can be highlighted:

- Viscoelastic behavior of the material during compaction and stress-relaxation. The highest recovery is observed after the first cycle.
- Increased thickness reduction with the increment of temperature, pressure, and cycles until a limit is reached. Temperature has a dominant effect on the thickness under the compaction threshold.
- Increased void content and max. void size with the increment of compaction reduction.
- Normalised thickness profile independent of the specimens' number of plies. Additionally, a similar final compaction ratio was observed among the number of plies studied.
- Compaction limit dependence on the plies' configuration and tape type. The complex interaction between the fibres has a dominant effect in comparison to the material viscosity.
- The nip point of the AFP process was replicated in this study. After the compaction limit is reached, it is suggested that the resin bleeds to the unconsolidated area, and thus, further cycles cause the presence of voids within the sample. This should be considered, depending on the number of layers deposited during the process to avoid the generation of voids, and thus, potentially reduce further debulking cycles.

These aspects can be considered for the actual AFP process and their various models to select the

adequate processing parameters. Nevertheless, some questions still need to be answered to continue process optimisation. Understanding the flow mechanism within the samples is crucial to favor the desired mechanism in the diverse stages of the process, including layup, debulking, and autoclave curing.

To exploit the results obtained during this work, it is crucial to understand the relation between the void content and the compaction of the material, since one of the most outstanding purposes of this study is the optimisation of the layup toward less debulking cycles by reducing the air entrapped within the laminate from an early process stage. Moreover, the degrees of freedom of processing parameters, such as the temperature, need to be considered further due to their influence on other prepreg properties, for example, the prepreg tack.

Among the study's main limitations, it is important to mention that both the compaction rate and time during the experiments are being overestimated due to the rheometer capabilities. During the AFP process, the values for these parameters are much lower. Thus, direct comparison and usage of the data for process optimisation needs to be adapted to realistic AFP conditions. Moreover, the influence of the compaction roller still needs to be investigated in further works. Lastly, the bulk-compaction simplification also deviates from the AFP process, in which each layer is compacted during deposition of the subsequent one. Therefore, the present study limits quantitative analysis of the results. Hence, the study is considered an initial indicator of the qualitative results.

Conclusions

The optimisation of automated process efficiency for prepreg materials can be carried out by understanding the compaction behavior of the material itself. This should also provide more information to predict the final laminate properties and select the adequate processing parameters to optimise the AFP process by potentially reducing further vacuum debulking or autoclave curing cycles.

Throughout this study, the compaction behavior was analysed on a lab-scale under controlled conditions. The results of this study regarding the compaction behavior of uncured thermoset prepreps showed that the thickness reduction of the specimens was strongly influenced by temperature until the compaction limit was approached (at ~50% reduction). No further compaction was observed above this temperature limit. The increase in pressure led to a compaction limit at lower temperatures. This effect shows good agreement with other studies [5, 9]. Once the compaction limit is reached

at specific processing conditions, further cycles may favor bleeding flow and the generation of voids. This effect may also be present during the AFP process due to similar boundary conditions regarding pressure, temperature, partial compaction, and cyclic behavior.

Further studies are needed to understand the relationship between void fraction and compressibility under actual AFP conditions to gain more insight into the compaction behavior that is not influenced by the bulk compaction carried out in this study.

Samples with crosswise layer configuration showed only 16.1% thickness reduction at 0.5 MPa and 55 °C, while unidirectional stacked samples showed a decrease of 51.7%. The influence of the number of layers on the qualitative thickness profile and the thickness reduction percentage were negligible. Final thickness reductions were 91.5, 83.2, 66.9, 51.7, 53.9, and 54.3% for the samples consisting of 2, 4, 8, 16, 24, and 32 layers. The effect of the tape type showed no a clear trend concerning the temperature. However, it is assumed that the compaction limit was not reached under the conditions investigated.

This study indicates the qualitative compaction behavior of the material. Nevertheless, further investigations to gain deeper insight into the compaction behavior of uncured thermoset prepreg under AFP conditions are necessary to determine the flow mechanism within the sample, analyse the void content in the samples after compaction, and evaluate the expansion in the width of the samples to confirm the contribution of the squeezing flow to the thickness reduction during the compaction cycles. Furthermore, the comparison of the material behavior in full-scale AFP conditions is crucial to determine the relationship with the controlled environment results and the ability to derive quantitative data for optimising the process. Moreover, the relation between the compressibility and void reduction during deposition needs to be analysed to exploit the potential decrease of debulking and autoclave curing steps.

Disclosure statement

The authors declared no potential conflicts of interest concerning the research, authorship, and publication of this article.

References

- [1] Lukaszewicz D, Potter K. Through-thickness compression response of uncured prepreg during manufacture by automated layup. *Proc Inst Mech Eng B J Eng Manuf.* 2012;226:193–202.

- [2] Lukaszewicz D, Ward C, Potter KD. The engineering aspects of automated prepreg layup: History, present and future. *Compos B Eng*. 2012;43:997–1009.
- [3] Blößl Y, Schledjewski R. A robust empirical model equation for the compaction response of textile reinforcements. *Polym Compos*. 2021;42(1):297–308.
- [4] Rogers TG. Squeezing flow of fibre-reinforced viscous fluids. *J Eng Math*. 1989;23(1):81–89.
- [5] Nixon-Pearson OJ, Belnoue J, Ivanov DS, et al. An experimental investigation of the consolidation behaviour of uncured prepreps under processing conditions. *J Compos Mater*. 2017;51:1911–1924.
- [6] Hubert P, Poursartip A. Aspects of the compaction of composite angle laminates: an experimental investigation. *J Compos Mater*. 2001;35(1):2–26.
- [7] Gutowski TG, Dillon G. The elastic deformation of lubricated carbon fiber bundles: comparison of theory and experiments. *J Compos Mater*. 1992;26:2330–2347.
- [8] Cai Z, Gutowski T. The 3-D deformation behavior of a lubricated fiber bundle. *J Compos Mater*. 1992;26:1207–1237.
- [9] Ivanov D, Li Y, Ward C, et al. Transitional behaviour of prepreps in automated fibre deposition processes. In: ICCM International Conferences on Composite Materials; 2013 July. International Committee on Composite Materials; 2013. p. 1381–1391.
- [10] Lichtinger R. Thermo-Mechanical coupled simulation of the thermoset automated fibre placement process [PhD dissertation]. Chair of Carbon Composites at the Technical University of Munich; 2015. mediaTUM. <https://mediatum.ub.tum.de/1244909>.
- [11] Engelhardt R, Irmanputra R, Brath K, et al. Thermoset prepreg compaction during automated fiber placement and vacuum debulking.pdf. *Proc CIRP*. 2019;85:153–158.
- [12] Belnoue J, Nixon-Pearson OJ, Ivanov D, et al. A novel hyper-viscoelastic model for consolidation of toughened prepreps under processing conditions. *Mech Mater*. 2016;97:118–134.
- [13] Naito Y, Nishikawa M, Mobuchon C, et al. Effect of rheological transitions in matrix resin on flow mechanism of carbon fiber/epoxy prepreg. *Compos A Appl Sci Manuf*. 2021;151:106612.
- [14] Sorba G, Binetruy C, Leygue A, et al. Squeeze flow in heterogeneous unidirectional discontinuous viscous prepreg laminates: experimental measurement and 3D modeling. *Compos A Appl Sci Manuf*. 2017;103:196–207.
- [15] Lukaszewicz D, Potter KD, Eales J. A concept for the in situ consolidation of thermoset matrix prepreg during automated lay-up. *Compos B Eng*. 2013;45(1):538–543.
- [16] Hexcel Corporation, Product data sheet HexPly 8552. n.d. 1–6.
- [17] Nairn JA. Effects carbon of fiber, matrix, fiber composite and interphase compression on strength. Contractor Report (CR). Document ID: 19940029731. Nasa Technical Reports Server; 1994.
- [18] Etchegaray Bello M, Engelhardt R, Drechsler K. Dataset for cyclic compaction-recovery behavior of CF/Epoxy/8552 multilayer samples. Technical University of Munich, mediaTUM; 2021. <https://doi.org/10.14459/2021imp1621517>.
- [19] Engelhardt R, Brath K, Ebel C, et al. Experimental analysis of the compaction behavior of thermoset prepreg tapes during automated fiber placement. ECCM 2018 - 18th Eur Conf Compos Mater. 2018:24–28. https://www.researchgate.net/publication/349213807_Experimental_Analysis_of_the_Compaction_Behavior_during_Thermoset_Automated_Fiber_Placement.